S.T. Yau High School Science Award

Research Report

The Team

Name of team member: Jamie Zhu
School: Eastlake High School
City, Country: Sammamish, United States

Name of supervising teacher: Medet Segizbayev, PhD
Job Title: Post-Doctoral Fellow
School/Institution: University of Ottawa
City, Country: Ottawa, Canada

Title of Research Report

Distance Dependent qE: Charge Transfer and Charge Transfer-Mediated Superexchange in a Chlorophyll *a* – Lutein Dimer

Date

September 12, 2026

Distance Dependent qE: Charge Transfer and Charge Transfer-Mediated Superexchange in a Chlorophyll *a* – Lutein Dimer

12 September 2026

Author: Jamie Zhu

High School: Eastlake High School

Washington, USA

Instructor: Medet Segizbayev, PhD

University of Ottawa

Ottawa, Canada

Distance Dependent qE: Charge Transfer and Charge Transfer-Mediated Superexchange in a Chlorophyll *a* – Lutein Dimer

Jamie Zhu

Abstract

In oxygenic photosynthesis, plants utilize specialized antenna complexes or light harvesting complexes (LHCII) to absorb sunlight and drive photosynthetic reactions which occur in reaction centers. However, the absorption of excess energy under high-light conditions risks the creation of toxic singlet oxygen, which causes photodegradation and DNA mutations. To safeguard the photosystem, plants employ Nonphotochemical Quenching (NPQ), specifically the fastest component known as energy dependent quenching (qE). This process dissipates excess excitation energy as heat before singlet oxygen can form. While the importance of qE is well investigated, the precise mechanisms of energy dissipation remain highly debated. Among the many proposed quenching mechanisms, this study investigates two theorized de-excitation pathways: charge transfer (CT) and Charge-Transfer (CT) mediated superexchange. We utilized computational frameworks to generate diabatic Hamiltonians, effective electronic coupling energy calculations, and quenching rates of the respective methods. Overall, at calculated intermolecular distances of 10.772, 11.772, 12.772, and 13.772 Å, the de-excitation rate of CT-mediated superexchange was higher than CT. Notably at the optimized bond distance of 12.772 Å, the rate of CT-mediated superexchange (2.04×10^{11} s^{-1}) was higher than CT (1.19×10^{4} s^{-1}). Across all calculated bond distances, the quenching rate of CT-mediated superexchange peaked at 11.772 Å. These findings indicate that CT-mediated superexchange relies on mixing of states due to thermodynamically unfavourability of CT. The results suggest that CT-mediated superexchange is more thermodynamically accessible; utilizing a mix of electronic states.

Keywords: *Light Harvesting Complex, Photosynthesis, Chlorophyll a, Lutein, Non-Photochemical Quenching, Excitation Energy, Computational Frameworks*

Acknowledgement

The subject of this research is a comparative analysis regarding Non-Photochemical Quenching (NPQ) and the de-excitation pathways a plant utilizes to dissipate harmful energies produced by photosynthesis, mainly under high intensity environments. This research idea was inspired by Berkelbach's paper on *Microscopic theory of singlet exciton fission. II. Application to pentacene dimers and the role of superexchange (2012).* Berkelbach applied his research towards Pentacene and I wanted to see how his theories would play out in another photosynthetic interaction, between Chlorophyll *a* and Lutein. In previous research papers that I read, the Chlorophyll *a* - Lutein interaction showed up multiple times as the primary focus of these experiments were directed upon. Thus, I wanted to bridge that gap with this research paper.

The idea of singlet fission and the theory of a quenching mechanism which involved mixing of singlet states intrigued me.

Rather than utilize open-source data, which were not easily accessible, we conducted our own experiments using common computation chemistry software. We used Avogadro, a widely used molecular visualization tool, and TeraChem, a GPU-accelerated computational chemistry package to run the calculations. The utility of Avogadro and TeraChem were necessary, as a physical experiment of singlet fission is difficult to assess due to the mechanism's extremely short lifetime.
To set up this experiment, I was given the Chl *a* – Lutein dimer by my advisor, which I subsequently optimized, resulting in the optimized distance of 12.772 Å. The process of perturbating the distances between each molecule involved the drawing of a fictitious bond between the central Magnesium

atom on the Chlorophyll *a a*nd the distal terminal carbon on the Lutein. Next, the distance between these two molecules were perturbed, resulting in the final four intermolecular distances. To compute the resulting output file generated by TeraChem, I wrote an agnostic python class that parsed the data and extracted useful results which made the final analysis easier.

One challenge I faced was the modelling of the Chlorophyll *a* – Lutein dimer. The research topic necessitated the examination of electronic interactions between these two molecules across various distances. During the process of increasing and decreasing the distances between the two molecules by increments of 1.0 Å, I ran into bond inconsistencies when modulating the bond distances past 10.772 Å and 13.772 Å. For example, Avogadro would visualize a double bond between a hydrogen and a carbon which is rather unlikely. Consequently, this limited the data range to only cover four calculated distances.

I would like to thank my advisor, Dr. Segizbayev, for his mentorship throughout the research process. With his support, I studied TeraChem calculations generated by Avogadro and wrote up my research results in this paper. His suggestions during the peer-review process removed inconsistencies with my writing and language. In addition, I am grateful for Dr. Taffet who allowed me to use his GPU-accelerated software to run my calculations which I independently analysed.

In this research process, I carried out the experiments regarding visualization of the Chlorophyll *a* – Lutein dimer, writing of TeraChem input scripts, analysis of resulting data, and authoring of research paper independently; without the help or usage of any AI tools. Thus, I am responsible for quality and integrity of this research paper.

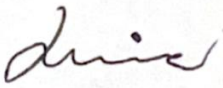
Commitments on Academic Honesty and Integrity

We hereby declare that we

1. are fully committed to the principle of honesty, integrity and fair play throughout the competition.
2. actually perform the research work ourselves and thus truly understand the content of the work.
3. observe the common standard of academic integrity adopted by most journals and degree theses.
4. have declared all the assistance and contribution we have received from any personnel, agency, institution, etc. for the research work.
5. undertake to avoid getting in touch with assessment panel members in a way that may lead to direct or indirect conflict of interest.
6. undertake to avoid any interaction with assessment panel members that would undermine the neutrality of the panel member and fairness of the assessment process.
7. observe the safety regulations of the laboratory(ies) where we conduct the experiment(s), if applicable.
8. observe all rules and regulations of the competition.
9. agree that the decision of YHSA is final in all matters related to the competition.

We understand and agree that failure to honour the above commitments may lead to disqualification from the competition and/or removal of reward, if applicable; that any unethical deeds, if found, will be disclosed to the school principal of team member(s) and relevant parties if deemed necessary; and that the decision of YHSA is final and no appeal will be accepted.

(Signatures of full team below)

x 

Name of team member: Jamie Zhu

x 

Name of supervising teacher: Medet Segizbayev, PhD

Table of Contents

Table of Contents

1. Introduction 1
2. Materials and Methods 3
   - 2.1 Usage of Quantum Calculation Tools and Geometry Optimization 3
   - 2.2 System Calculation Parameters 4
   - 2.3 Agnostic Python Class to Parse TeraChem Output Script 6
3. Results 7
   - 3.1 Diabatic Energy Gap and Electron Coupling Strength on Distance (10.772 Å – 13.772 Å) 7
   - 3.2 Coupling between electronic transfer states ($\boldsymbol{Lut+/Chl-}$) 9
   - 3.3 State Composition and Final Diabatic Energy of Five Lowest Singlet States 10
   - 3.4 Distance Dependence of Quenching Rates (10.772 Å – 13.772 Å) 12
4. Discussion 14
   - 4.1 Dominance of CT/TT Mixing at 12.772 Å Distance 14
   - 4.2 Trends in Quenching Rates 14
   - 4.3 Relationship between Thermodynamic Favorability and Rate of Quenching 15
   - 4.4 Limitations 16
5. Conclusion 16

References 18

1. Introduction

Operating as the primary sites of oxygenic photosynthesis, photosystems must balance efficient absorption and funneling of solar energy while also rapidly preventing the formation of harmful species under high-energy stress. The system accomplishes this through the integration of three key structures: LHCII, the reaction centers, and the carotenoid quenchers embedded throughout the system (Croce, 2014). Within LHCII, energy is transferred amongst pigments, generally traveling to lower-energy states nearer the reaction sites through excitonic and resonance energy-transfer processes.

While this process proves viable under normal circumstances, when a light-harvesting pigment is consistently bombarded with high-energy photons, the resulting excited state configuration can be maintained for an extended period. This stems from the formation of chlorophyll (Chl) *a* triplet state which, when coming in contact with oxygen, forms singlet oxygen: a process that can lead to photoinhibition (Niyogi, 2013; Pinnola & Bassi, 2018). To prevent this damage, plants use carotenoids to dissipate the excess excitation (Niyogi, 2013; Pinnola & Bassi, 2018). In this study, we investigated the photoprotective interactions between Chl *a,* the primary excitation energy donor and the carotenoid lutein (Lut), the primary quencher of Chl *a* excitation (Croce, 2014). These two molecules are common amongst various photosystems in photosynthetic organisms. Lut's flexible conjugated Carbon-Carbon single and double bond as well as its short-lived S_1 state allow it to trap the excess energy and dissipate the energy as heat.

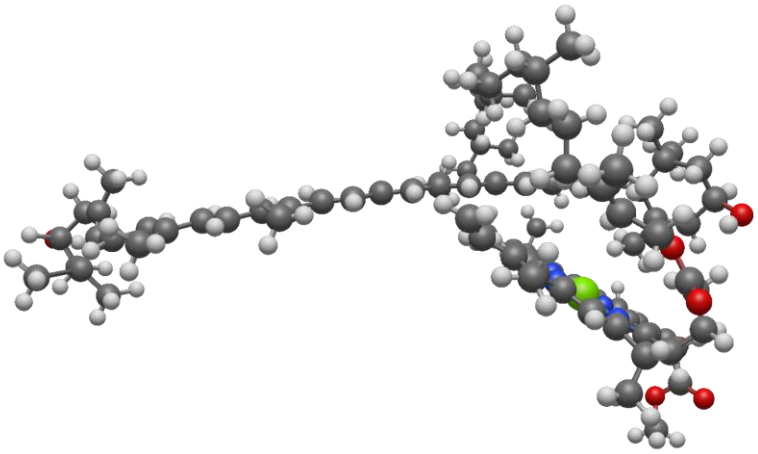


Figure 1. A visualization of the two-molecule system of the carotenoid Lutein and Chlorophyll *a*. Magnesium is in green; oxygen in red; nitrogen in blue, carbon in dark gray, and hydrogen in white. Chlorophyll *a* contains a Magnesium atom at the center of a porphyrin ring. The Lutein molecule contains two six-membered rings connected by a conjugated carbon-carbon single and double bond chain. Each ring contains three methyl groups and one -OH group.

While the photophysical mechanisms Lut employs once excited have been extensively studied, the methods to transfer energy remains questioned. Currently, the scientific community is divided amongst two possible mechanisms: CT and CT-mediated superexchange (Ahn et al., 2008; Berkelbach et al., 2012).

CT is a sequential process where a ground state electron from a carotenoid electron-donor is transferred to the hole generated by an exciton. This creates a radical ion pair ($Lut^{(+)}$/ $Chl^{(-)}$) where Lut is oxidized and Chl *a* is reduced. Thereafter, the excited electron undergoes charge recombination with the lutein cation. The majority of the energy is dissipated during charge recombination while the remaining is trapped within the Lut S_1 state (Burdett et al., 2010). Previous research suggests that the lifetime of this charge-separation lasts only 10 picoseconds, a small fraction of the entire process's lifetime of ~277 picoseconds (Cupellini, 2020; Liu et al., 2004). Despite CT being significantly briefer compared to other methods such as triplet-triplet and Förster

resonance energy transfer (FRET), it is debatable whether this process remains the most viable pathway. This is due to the necessity to overcome a large energy gap to reach this reaction intermediate.

Previous models showed that the conditions for efficient CT must require the CT state to be positioned between singlet state and a separate, triplet-triplet (TT) state of excitation. In addition, Zimmerman et al. (2011) revealed that a charge transfer (CT) state is thermodynamically unviable due to an energy gap of ~ 300 meV between relevant singlet and CT states. This suggests the necessity for a lower-lying method of energy transfer in which the higher-energy CT state mediates superexchange. CT-mediated superexchange, is like CT except the two-step electron transfer occurs simultaneously. This process occurs when the wavefunctions of the respective molecules strongly overlap, allowing the electrons to tunnel through. While Dexter energy transfer occurs at close proximity, the "virtual" CT state aids the mechanism at longer distances as well (Cupellini, 2020). In Berkelbach et al. (2013), the researchers theorized that $E_{(CT)} - E_{(TT)} \gg E_{(S1)} - E_{(TT)}$.

For both CT and CT-mediated superexchange, there has been much discussion on the varying importance of each method of quenching the dissipation of harmful energies. Despite the underlying research done, the specific interaction has not been thoroughly evaluated between Lut and Chl *a* (Pinnola & Bassi, 2018; Wahadoszamen et al., 2012). This study aims to apply previous theoretical models to compare the calculated kinetic rates of each method in a Chl *a* – Lut dimer, specifically evaluating the quenching rates at various chosen intermolecular distances.

2. Materials and Methods

2.1 Usage of Quantum Calculation Tools and Geometry Optimization

Our work builds upon that of (Berkelbach et al., 2012); applying their findings and models to the de-excitation patterns of Chlorophyll *a* and Lutein. We conducted our studies using a combination of Avogadro, an open-source 3D visualization tool, and TeraChem, a Graphics Processing Unit (GPU)-accelerated quantum chemistry software program (Seritan, 2021). Our model represents a simplified Chl *a* – Lut dimer intended to investigate electronic interactions in isolated conditions (specific basis sets and geometry optimization methodology are detailed in Section 2.2).

Through this framework we modeled the quenching of Chl *a* excitation energy following the optically allowed absorption of visible-energy photons. Our *ab initio* model contains a 98-atom Lut carotenoid and a 137-atom Chl *a*, a primary photosynthetic pigment. These two molecules represent the bare minimum required to evaluate the interplay of carotenoid – chlorophyll pairs in nonphotochemical quenching (Liu et al., 2004). This process was performed to minimize undesirably high dimensionality, lowering the computational cost. Running the molecular dimer is our basis for the final dissipation rate of the respective methods.

2.2 System Calculation Parameters

Quantum calculations were then performed under the basis set cc-pVDZ, otherwise known as Correlation-Consistent Polarized Valence Double-Zeta, which allows the approximation of molecular orbitals using polarization functions. To illustrate the electron-electron interactions, the dimer was run under the wPBEh method to treat short and long interelectronic distance electron transfer seperately. A range-separation parameter of 0.15 $Bohr^{-1}$ allows for the smooth transition in exchange from Density Functional Theory (DFT) to Hartree Fock. While the overall charge of the dimer was set to neutral, CT states reflected molecular cation – anion combinations (Lut^{+}/Chl^{-}) while retaining an overall charge of zero.

To investigate the influence of the thermodynamic and electronic interplay, we processed the respective data points using the non-adiabatic Marcus Theory equation under the following

parameters. We implemented a temperature of 298 K and self-reorganization energy of 0.35 eV. A reorganization energy of 0.35 was implemented to model the rigidity of each molecule and the hydrophobic environment in which the dimer resides within a plant.

The resulting 5×5 Hamiltonian of matrix elements generated by TeraChem describes the diabatic site energies and off-diagonal coupling elements of selected electronic states. $E(S_1S_0)$ represents the energy of a Chl-localized exciton, $E(S_0S_1)$ represents the energy of a Lut-localized exciton, $E(T_1T_1)$ represents the TT state, $E(CA)$ represents the energy of Chl^+/Lut^- and $E(AC)$ represents the energy of Lut^+/Chl^-.

$$\hat{H}_{el} = \begin{pmatrix} E(S_1S_0) & 0 & 0 & 116 & 145 \\ 0 & E(S_0S_1) & 0 & 145 & 116 \\ 0 & 0 & E(T_1T_1) & -152 & 133 \\ 116 & 145 & -152 & E(CA) & 0 \\ 145 & 116 & 133 & 0 & E(AC) \end{pmatrix}$$

Figure 2. This is a sample Hamiltonian generated by TeraChem. Along the diagonal lie the diabatic energies of various excited states, locally excited states (S_1S_0) and (S_0S_1), the triplet-triplet state (T_1T_1), and charge transfer (CA) and (AC). The off-diagonal elements represent the electronic coupling energies between excited states.

The diagonal elements model the energies of the two locally excited (LE) states of Chl then Lut followed by one TT state and two CT states. Units are expressed as labeled.

In addition, to calculate the effective electronic coupling energies, V_{eff} of the two mechanisms--CT and CT-mediated superexchange--we applied the second order perturbation theory (McConnell, 1961):

$$V_{\text{eff}} = \frac{V_{\text{LE, CT}} \times V_{\text{CT, TT}}}{\Delta E} \tag{1}$$

The initial LE state is that of the Chl-localized exciton while the CT state that is the lowest and most dominant one is a Lut^{+}/Chl^{-} radical ion pair. The $V_{\text{LE, CT}}$ (the coupling energy between LE and CT states) and $V_{\text{CT, TT}}$ (the coupling energy between CT and TT states) were parsed directly from the generated Hamiltonian. ΔE represents the energy difference between the mediating CT state and the localized excited state. This equation will allow us to derive the electronic coupling values for CT-mediated superexchange and compare them with the effective electronic coupling values generated by TeraChem.

2.3 Agnostic Python Class to Parse TeraChem Output Script

Following the quantum mechanical calculations, we developed a Python *EXCANALYSIS* class to parse the resulting TeraChem output files. The objective was to extract the electronic-coupling energies and state energy gaps to subsequently calculate the rates of each quenching mechanism. We applied the Marcus Theory for non-adiabatic electron transfer, which yielded the transfer frequencies in Hertz (Marcus, 1993). This equation approximates the rates of a quenching method rather than generating experimentally measured frequencies.

$$k_{CT} = \frac{2\pi}{\hbar} \left|V_{eff}\right|^2 \frac{1}{\sqrt{4\pi\lambda k_b T}} \exp\left(-\frac{(\Delta E + \lambda)^2}{4\lambda k_b T}\right) \tag{2}$$

We repeated this calculation multiple times, performing rigid-body translations by increments of 1.0

Å to systematically examine how each coupling method would perform at different distances. The intermolecular distance varied from 10.772 to 13.772 Å with 12.772 Å corresponding to the optimized geometry distance, measured between the central Mg atom on the Chl *a* and the distal terminal carbon on the lutein. To obtain this optimized geometry distance of 12.772 Å, we utilized Avogadro's optimization tool. An increment of 1.0 Å was chosen to allow for distortion of electron clouds. The geometry of the dimer was not reoptimized after each perturbation.

The examination of deactivation rate at various distances is important to mimic natural flexibility within individual light-harvesting complexes where pigment-pigment distances can be affected by environmental factors (Cupellini, 2020; Liguori, 2015). Because the activation of a certain method in this interaction is distance-dependent, a range of 3 Å was chosen to sufficiently cover the tail end of electron coupling when the photosystem is compressed or stretched. Past this range, the fictitious bond creates unwanted side effects regarding bond assignment. For example, a further extension past this barrier causes confusion within Avogadro's automated engine assigning two carbons to bond with one hydrogen. A separate .csv file was introduced to store the activated methods of quenching at the various distances.

The Python class used to synthesize the TeraChem output is accessible here:
https://github.com/jamie-zhu-98/EXCANALYSIS/blob/main/EXCANALYSIS.py

3. Results

3.1 Diabatic Energy Gap and Electron Coupling Strength on Distance (10.772 Å – 13.772 Å)

We performed the calculation on 156 and 241 occupied molecular orbitals in Chl *a* and Lut, respectively. The Highest Occupied Molecular Orbital – Lowest Unoccupied Molecular Orbital (HOMO-LUMO) energy gap was calculated to be 4.998 eV for Chl *a*nd 4.793 eV for Lut.

Table 1. The energy gap between locally excited and charge transfer states and the effective electronic coupling energy values at inspected distances (10.772 - 13.772 Å). Energies are represented in terms of atomic units (a.u.).

Intermolecular Distance between Chlorophyll and Lutein (Å)	Locally Excited – Charge Transfer state energy gap	V_{eff} of Charge Transfer (a.u.)
10.772	0.035561 a.u.	-6.20 x 10^-5
11.772	0.035696 a.u.	2.00 x 10^-6
12.772	0.033443 a.u.	-5.00 x 10^-6
13.772	0.035563 a.u.	-2.00 x 10^-6

Evaluation of the diabatic Hamiltonian matrices reveals two LE states, two CT states, and one TT state. There is one LE state for each molecule and two radical-ion pairs, Chl^{+}/Lut^{-} and Lut^{+}/Chl^{-}. As Lut acts as the primary quencher of Chl excitation, our analysis focused on the Lut^{+}/Chl^{-} state due to its lower calculated diabatic energy. Notably, at 12.772 Å, the optimized distance, the energy gap between LE state and the primary CT state was calculated to be ~0.033443 a.u or ~910 meV.

3.2 Coupling between electronic transfer states (Lut^{+}/Chl^{-})

Table 2. The TeraChem computations for locally excited to charge transfer coupling, charge transfer to triplet-triplet coupling. The included LE-CT energy gap from Table 1 to determine the effective electronic coupling energies V_{eff} at chosen distances for Charge-Transfer mediated superexchange. The V_{eff} value was calculated using McConnell's second order perturbation theory. All values are in atomic units (a.u.).

Intermolecular Distance between Chlorophyll and Lutein (Å)	LE/CT Coupling Energy	CT/TT Coupling Energy	LE/CT Energy Gap (ΔE)	V_{eff} of CT-mediated superexchange (a.u)
10.772	-0.00070032463281	0.0005789103586	0.035561 a.u.	-1.14×10^{-5}
11.772	0.00063078014019	0.0016354709293	0.035696 a.u.	2.89×10^{-5}
12.772	1.4363513535e-05	0.00068771348972	0.033443 a.u.	2.95×10^{-7}
13.772	7.8108956659e-06	-8.0481308787e-05	0.035563 a.u.	-1.77×10^{-8}

The intermolecular distance of 11.772 Å produced the highest effective electronic coupling energy amongst sampled distances.

3.3 State Composition and Final Diabatic Energy of Five Lowest Singlet States

Table 3. Composition of excitons based on the mixing of LE, CT, and TT characters depicting that of 12.772 Å results. These singlet states represent the five lowest-energy excited singlet states. Percentages may not amount to one hundred due to system rounding errors. Mixing is quantified in percentage units.

Five Lowest Singlet States (Lut+/Chl-)	Percent LE	Percent CT	Percent TT	Final Diabatic Energy (eV)
S_1	100	0	0.00	2.87
S_2	100	0	0.10	2.29
S_3	0	10.2	89.8	3.24
S_4	0	92.4	7.6	3.64
S_5	0	97.4	2.6	3.19

For the singlet state composition of the 235-atom dimer, we collected the various mixing of LE, CT, and TT energies. A high percentage makeup of a LE, CT, or TT percentage translates to high probability to undergo the respective methods of quenching. S_1 and S_2 are predominantly LE with

little CT/TT mixing. The S_4 and S_5 singlet states both exhibit strong characteristics of a radical ion pair with CT character of 92.4% and 97.4% respectively. On the other hand, the S_3 state illustrates the inverse relationship, a 10.2% CT character and 89.8% TT character. Illustrated below are the singlet state composition values for the other distances, 10.772 Å, 11.772 Å, 13.772 Å.

Table 4. Composition of excitons based on the mixing of LE, CT, and TT characters depicting that of 10.772, 11.772, 13.772 Å results. These singlet states represent the five lowest-energy excited singlet states. Percentages may not amount to one hundred due to system rounding errors. Mixing is quantified in percentage units.

Intermolecular Distance (Å)	Five Lowest Singlet States (Lut+/Chl-)	Percent LE	Percent CT	Percent TT	Final Diabatic Energy (eV)
10.772	S_1	98.5	1.40	0.00	2.88
	S_2	88.7	11.3	0.10	2.29
	S_3	1.10	31.3	67.6	3.18
	S_4	10.9	89.1	0.10	3.38
	S_5	0.80	67.0	32.2	3.25
11.772	S_1	99.7	0.30	0.00	2.88
	S_2	96.0	3.90	0.10	2.29

	S_3	3.00	62.40	34.5	3.21
	S_4	0.80	35.40	64.0	3.55
	S_5	0.40	98.20	1.40	3.26
13.772	S_1	100.0	0.00	0.00	2.29
	S_2	99.90	0.10	0.00	2.88
	S_3	0.00	0.3	99.7	3.25
	S_4	0.10	99.9	0.00	3.45
	S_5	0.00	99.7	0.30	3.63

3.4 Distance Dependence of Quenching Rates (10.772 Å – 13.772 Å)

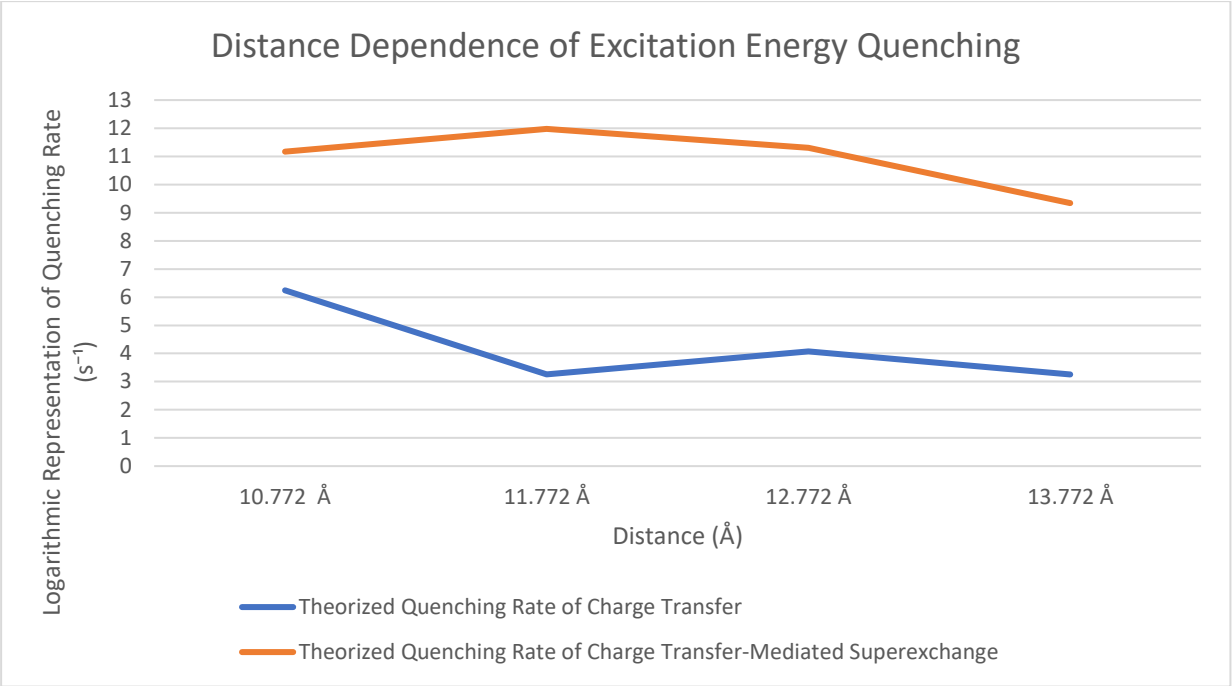


Figure 3. An illustration of the relationship between quenching rates of Charge Transfer and Charge Transfer-mediated superexchange and the intermolecular distance between Chlorophyll *a* and Lutein. The y-axis models a logarithmic scale of the quenching rate in s^{-1}. Along the x-axis are the various distances, starting from 10.772 Å, increasing by increments of 1 Å, and ending at 13.772 Å.

The calculated rate was the largest at 11.772 Å amongst the four tested geometries. The fluctuations are proportional to the $|V_{\text{eff}}|^2$ value found in Table 1. These fluctuations correlate to the effective electron coupling energies found in Table 1 where similarly they are highly sensitive to changes in distances.

$$Q = \frac{Rate_{Charge\ Transfer-mediated\ superexchange}}{Rate_{Charge\ Transfer}} \quad (3)$$

Despite the decrease in *Q* when the distance was shortened to 10.772 Å from 11.772 Å, the CT-mediated superexchange was found to be several orders of magnitude larger. *Q* is a dimensionless ratio between the rates of CT-mediated superexchange and CT.

4. Discussion

4.1 Dominance of CT/TT Mixing at 12.772 Å Distance

At the optimized geometry of 12.772 Å, each singlet state exhibited distinct state compositions. Analysis focused on the three transfer states: the S_3 state exhibits a high TT character of 89.8% and a CT character of 10.2%. Conversely, S_4 and S_5 illustrate the inverse relationship of S_3, reporting 92.4% CT and 97.4% CT respectively. Among these CT and TT states, S_5 represents the lowest-energy CT intermediate, corresponding to a Lut^+/Chl^- radical ion pair. Its final diabatic energy of 3.19 eV is lower than the other CT intermediate, S_4, which has a final diabatic energy of 3.64 eV. We noticed that the energy gap between the lowest energy LE state (S_2) and S_5 is calculated to be ~910 meV. This energy gap matched the HOMO – LUMO gap generated by TeraChem. However, such a large energy gap between S_2 and S_5 states highlights the unlikeliness of populating this charge-transfer intermediate. The calculated gap of ~910 meV is significantly higher than the 300 meV (0.300 eV) upper bound for thermal activation proposed in (Zimmerman et al., 2011). While Zimmerman's studies were applied to a different set of molecules, at standard temperature there is only around 23-25 meV of thermal energy available. Therefore, the CT state remains thermodynamically unviable.

4.2 Trends in Quenching Rates

At relaxed geometry, the calculations found that the rate of CT-mediated superexchange is $2.04 \times 10^{11}\ s^{-1}$ compared to $1.19 \times 10^{4}\ s^{-1}$ of CT energy exchange. Despite the perturbation of intermolecular distances, the results showed that CT-mediated superexchange had a higher

calculated rate. Upon further examination of the rates, we found that the calculated rate of CT-mediated superexchange significantly increased upon a distance decrease of 1 Å, from 12.772 Å to 11.772 Å. This increase in quenching rate can be attributed to a dramatic increase in effective electronic coupling energy from 2.95×10^{-7} a.u. to 2.89×10^{-5} a.u., Table 2.

A decrease in rate frequency occurred when an increase of 1 Å towards the distance was applied. At the two endpoints, the transfer frequency for CT-mediated superexchange at 13.772 Å reached $2.19 \times 10^{9} s^{-1}$, 1.2×10^{6} times faster than CT. At 10.772 Å the transfer rate reached $1.48 \times 10^{11}\ s^{-1}$ (8.4×10^{4} times higher than CT). This demonstrates the theoretical dominance of the simultaneous electron exchange pathway across multiple geometries. The data showed a significantly faster rate of quenching for CT-mediated superexchange versus CT. While the four sampled distances did not exhibit an exponential decay, further calculations at various distances are necessary to make certain conclusions about the data. We hypothesize that the non-exponential fluctuations are due to the structure entanglement between the two molecules as Chl *a*'s antenna structure wraps around the conjugated carbon chain of the Lutein, facilitating second-order wavefunction mixing, though a quantitative model would be necessary to confirm this interpretation.

Although the value of *Q* (See Equation 3) decreased to 10.772 Å compared to 11.772 Å, the superexchange method remained multiple orders of magnitude higher. This drop can be attributed to the overlap between positive and negative nodes of the two fragments at such proximity.

4.3 Relationship between Thermodynamic Favorability and Rate of Quenching

In Table 3, while the S_5 is the lowest energy individual transfer state, it remains thermodynamically unfavorable. Because this excited state is blocked, our calculations theorize that the dimer must rely on mixing of singlet states to quench the harmful energy. While the energy of S_5 is appreciably high, it can still mediate the transfer as it is never fully populated. In addition, CT requires substantial

electronic coupling but often the two molecules exhibit very weak coupling energies because the orbitals do not strictly align.

4.4 Limitations

Our model contains a few limitations. First, our studies were conducted in an isolated Chl *a* – Lut dimer whereas in real photosynthetic organisms, the two molecules would sit on the antenna within an LHCII. The absence of other molecules in the protein scaffold which can affect the diabatic site energies and coupling strengths are not captured. In addition, the quenching rates rely on a fixed reorganization energy to evaluate the dimer across only four intermolecular distances. Furthermore, we noted that the Marcus Theory relies on weak donor-acceptor coupling while our Chl *a* – Lut dimer can enter a stronger coupling geometry. Therefore, a more accurate method to calculate quenching rates is necessary. Consequently, the quantitative calculations generated using this model should not be interpreted as specific de-excitation rates. Instead, this model should act as a insight into comparative analysis of CT-mediated superexchange and CT.

5. Conclusion

With the help of modern computational tools, this study has shown that photoprotective quenching with the mediated-superexchange produces a higher calculated quenching rate than pure Charge Transfer within an isolated Chl *a* – Lutein dimer. We investigated the interactions that take place between abundant and important molecules that exist in this photosynthetic process. This finding puts into context the findings formulated in Berkelbach et al. (2013) by examining a frequent interaction between Chl *a* and lutein. By altering the molecular distances between the optimized fragment geometries, we showed CT-mediated superexchange maintains a higher calculated rate. In addition, we showed that while Charge Transfer may be the most favorable individual singlet state,

CT-mediated superexchange relies on the mixing of individual singlet states to contribute effective coupling. Our results show that a low-lying intermediate does not need to be appreciably populated for physical quenching to occur, rather the system can rely on a virtual intermediate to accurately transfer the energies. These findings may inform further investigation in the field of creating artificial photosynthetic devices, termed in Croce et al. (2014). Understanding the importance of CT-mediated superexchange can eventually offer insights to developing a low-energy method to safely reduce the negative effects of harmful excitation (Johnson et al., 2010; Lee et al., 2009).

References

Ahn, T. K., Avenson, T. J., Ballottari, M., Cheng, Y.-C., Niyogi, K. K., Bassi, R., & Fleming, G. R. (2008). Architecture of a Charge-Transfer State Regulating Light Harvesting in a Plant Antenna Protein. *Science*, *320*(5877), 794–797. https://doi.org/10.1126/science.1154800

Berkelbach, T. C., Hybertsen, M. S., & Reichman, D. R. (2012). *Microscopic theory of singlet exciton fission. II. Application to pentacene dimers and the role of superexchange*. https://doi.org/10.1063/1.4794427

Burdett, J. J., Müller, A. M., Gosztola, D., & Bardeen, C. J. (2010). Excited state dynamics in solid and monomeric tetracene: The roles of superradiance and exciton fission. *The Journal of Chemical Physics*, *133*(14), 144506. https://doi.org/10.1063/1.3495764

Croce, R. (2014). Natural strategies for photosynthetic light harvesting. *Nature Chemical Biology*, *10*(7), 492–501. https://doi.org/10.1038/nchembio.1555

Cupellini, L. (2020). Charge transfer from the carotenoid can quench chlorophyll excitation in antenna complexes of plants. *Nature Communications*, *11*(1), 662. https://doi.org/10.1038/s41467-020-14488-6

Dall'Osto, L. (2017). Two mechanisms for dissipation of excess light in monomeric and trimeric light-harvesting complexes. *Nature Plants*, *3*, 17033. https://doi.org/10.1038/nplants.2017.33

Holt, N. E., Zigmantas, D., Valkunas, L., Li, X.-P., Niyogi, K. K., & Fleming, G. R. (2005). Carotenoid Cation Formation and the Regulation of Photosynthetic Light Harvesting. *Science*, *307*(5708), 433–436. https://doi.org/10.1126/science.1105833

Johnson, J. C., Nozik, A. J., & Michl, J. (2010). High Triplet Yield from Singlet Fission in a Thin Film of 1,3-Diphenylisobenzofuran. *Journal of the American Chemical Society*, *132*(46), 16302–16303. https://doi.org/10.1021/ja104123r

Khokhlov, D., & Belov, A. (2019). Ab initio model for the chlorophyll-lutein exciton coupling in the LHCII complex. *Biophysical Chemistry*, *246*, 16–24.

Lee, J., Jadhav, P., & Baldo, M. A. (2009). High efficiency organic multilayer photodetectors based on singlet exciton fission. *Applied Physics Letters*, *95*(3), 033301. https://doi.org/10.1063/1.3182787

Liguori, N. (2015). From light-harvesting to photoprotection: Structural basis of the dynamic switch of the major antenna complex of plants (LHCII). *Scientific Reports*, *5*, 15661. https://doi.org/10.1038/srep15661

Liu, Z., Yan, H., Wang, K., Kuang, T., Zhang, J., Gui, L., An, X., & Chang, W. (2004). Crystal structure of spinach major light- harvesting complex at 2.72 ˚A resolution. *Nature*, *428*(6980), 287–292. https://doi.org/10.1038/nature02373

Marcus, R. (1993). Electron transfer reactions in chemistry. Theory and experiment. *Reviews of Modern Physics*, *65*(3), 599–610. https://doi.org/10.1103/RevModPhys.65.599

McConnell, H. M. (1961). Intramolecular Charge Transfer in Aromatic Free Radicals. *The Journal of Chemical Physics*, *35*(2), 508–515. https://doi.org/10.1063/1.1731961

Niyogi, K. K. (2013). Evolution of flexible non-photochemical quenching mechanisms that regulate light harvesting in oxygenic photosynthesis. *Current Opinion in Plant Biology*, *16*(3), 307–314. https://doi.org/10.1016/j.pbi.2013.03.011

Pinnola, A., & Bassi, R. (2018). Molecular mechanisms involved in plant photoprotection. *Biochemical Society Transactions*, *46*(2), 467–482. https://doi.org/10.1042/BST20170307

Ruban, A. V. (2018). Light harvesting control in plants. *FEBS Letters*, *592*(18), 3030–3043. https://doi.org/10.1002/1873-3468.13111

Seritan, S. (2021). TeraChem: A cloud-native quantum chemistry software. *WIREs Computational Molecular Science*, *11*(2), e1494. https://doi.org/10.1002/wcms.1494

Wahadoszamen, Md., Berera, R., Ara, A. M., Romero, E., & Van Grondelle, R. (2012). Identification of two emitting sites in the dissipative state of the major light harvesting antenna. *Phys. Chem. Chem. Phys.*, *14*(2), 759–766. https://doi.org/10.1039/C1CP23059J

Zimmerman, P. M., Bell, F., Casanova, D., & Head-Gordon, M. (2011). *Mechanism for Singlet Fission in Pentacene and Tetracene: From Single Exciton to Two Triplets*. *133*(49), 19944–19952. https://doi.org/10.1021/ja208431r